Published OnlineFirst July 7, 2009; DOI: 10.1158/0008-5472.CAN-08-0289

Analysis of the Human Cancer Glycome Identifies a Novel Group of Tumor-Associated *N*-Acetylglucosamine Glycan Antigens

Tero Satomaa,[1] Annamari Heiskanen,[1] Iréne Leonardsson,[4] Jonas Ångström,[4] Anne Olonen,[1] Maria Blomqvist,[1] Noora Salovuori,[1] Caj Haglund,[2] Susann Teneberg,[4] Jari Natunen,[1] Olli Carpén,[3,5] and Juhani Saarinen[1]

[1]Glykos Finland Ltd.; Departments of [2]Surgery and [3]Pathology, University of Helsinki and Helsinki University Central Hospital, Helsinki, Finland; [4]Department of Medical Biochemistry and Cell Biology, Göteborg University, Göteborg, Sweden; and [5]Department of Pathology, University of Turku and Turku University Hospital, Turku, Finland

Abstract

The cell surface is covered by a dense layer of protein- and lipid-linked glycans. Although it has been known that distinct glycan structures are associated with cancer, the whole spectrum of cancer-associated glycans has remained undiscovered. In the present study, we analyzed the protein-linked cancer glycome by matrix-assisted laser desorption/ionization time-of-flight mass spectrometric glycan profiling of cancer patient tissue samples. In lung cancer, we detected accumulation of a novel group of tumor-associated glycans. These protein-linked glycans carried abnormal nonreducing terminal β-*N*-acetyl-D-glucosamine (GlcNAc) residues. A similar phenomenon was also detected in structural analyses of tumor-derived glycosphingolipids. This showed that glycan biosynthesis may dramatically change in cancer and that direct glycome analysis can detect the resulting marker glycans. Based on the structural knowledge, we further devised a covalent labeling technique for the detection of GlcNAc-expressing tumors with a specific transferase enzyme. In normal tissues, terminal GlcNAc antigens are capped by galactosylation. Similarly to common cancer-associated glycan antigens T, Tn, and sialyl-Tn, the newly discovered GlcNAc antigens result from incomplete glycosylation. In conclusion, the identified terminal GlcNAc glycans should be recognized as a novel class of tumor markers. [Cancer Res 2009;69(14):5811–9]

Introduction

Protein- and lipid-linked carbohydrate structures, glycans, cover the surfaces of all human cells. Glycans are involved in the normal functions of multicellular organisms, and their structures change in cancer (1). Glycans associated with malignant transformation include various glycolipid structures (2); T, Tn, and sialyl-Tn mucin antigens (3, 4); and β1,6-branched complex *N*-glycans (5). Some glycans have already been taken into clinical development of cancer immunotherapies (6) and, for example, the glycan antigen sialyl Le^a (CA 19-9) is used in clinical cancer diagnostics. Specific glycans directly contribute to cancer progression (e.g., by promoting cancer metastasis and by modulating growth factor receptor activities; refs. 7, 8).

Previous studies of cancer-associated glycans have usually focused on single structures instead of the whole cancer glycome—the total spectrum of glycan structures present in cancer cells and tissues. In general, the normal human glycome is poorly understood, although it has been estimated that 1% of the human genome is involved in glycan biosynthesis (9). Characterization of the complete human glycome is under way. Further, glycomic analyses of cancer patient sera have revealed new cancer biomarkers (10). To directly compare the total protein-linked glycomes of normal human tissues and malignant tumors, we applied mass spectrometric profiling of protein-linked glycans and thin-layer chromatographic analysis of lipid-linked glycans to cancer patient tissue samples. The results show that the protein-linked glycomes of malignant tumors differ significantly from those of normal human tissues.

Materials and Methods

Tumor specimens. Tissue material was obtained from cancer surgery. Tumor specimens and normal tissue from the same organ were fixed in formalin and embedded in paraffin for routine diagnostic purposes. The normal morphology of the normal tissues was further verified before inclusion of the cases to the study. The tumor types included small-cell lung carcinoma, lung adenocarcinoma, renal cell carcinoma, lobular and ductal breast carcinomas, ovarian adenocarcinoma, colon carcinoma, pancreatic adenocarcinoma, gastric adenocarcinoma, hepatocellular carcinoma, and laryngeal squamous cell carcinoma.

Glycan isolation and purification. For glycan isolation, several 20-μm-thick sections were cut from paraffin blocks containing either tumor or normal tissue. The amount of tissue was at least 1 mm^3 in the present experiments. The samples were deparaffinized with xylene with ethanol-water series according to standard procedures. Protein-linked glycans were detached in nonreductive β-elimination conditions by incubation in concentrated ammonia and saturated ammonium carbonate at 60°C for 1 to 2 d, essentially as described (11). The detached reducing glycans were purified by a series of precipitation-extraction and solid-phase extraction chromatography steps. The isolated glycans were dissolved in water and prepurified by precipitating them with 80% to 90% (v/v) aqueous acetone at −20°C and then extracting them from the precipitate with 60% (v/v) ice-cold methanol essentially as described (12). The glycans were then passed in water through a combined solid-phase extraction column with strong cation-exchange resin (AG-50W, Bio-Rad) on top of C_{18} silica (BondElut, Varian). The collected flow-through was absorbed to solid-phase extraction column of porous graphitized carbon (Carbograph, Alltech) based on a previously described method (13). The carbon column was washed with water, after which the neutral glycans were eluted with 25% acetonitrile in water (v/v) and the sialylated glycans with 0.05% (v/v) trifluoroacetic acid in 25% acetonitrile in water (v/v). The sialylated glycans were further purified by adsorbing them in *n*-butanol/ethanol/water (10:1:2, v/v) to

Note: Supplementary data for this article are available at Cancer Research Online (http://cancerres.aacrjournals.org/).

T. Satomaa and A. Heiskanen contributed equally to this work.

Requests for reprints: Tero Satomaa, Glykos Finland Ltd., Viikinkaari 6, FIN-00790 Helsinki, Finland. Phone: 35-85-0525-5871; Fax: 35-89-3193-6341; E-mail: tero.satomaa@glykos.fi.

doi:10.1158/0008-5472.CAN-08-0289

Published OnlineFirst July 7, 2009; DOI: 10.1158/0008-5472.CAN-08-0289

microcrystalline cellulose in a miniaturized chromatography column (~10 μL), washing with the same solvent, and eluting by 50% ethanol/water (v/v). Final purification step was done with graphitized carbon packed into minicolumns (14).

Each of the purification steps in the glycan isolation procedure was validated with standard glycan mixtures and mass spectrometric analysis before and after purification step to ensure uniform glycan purification. The reproducibility of the procedure was validated by subjecting a human tissue sample to analysis by five different persons. The results were highly comparable, especially by the terms of detection of individual glycan signals and their relative signal intensities, showing that the reliability of the present method is suitable for comparing analysis results from different samples.

Mass spectrometric profiling. Matrix-assisted laser desorption/ionization time-of-flight (MALDI-TOF) mass spectrometry was done with a Voyager-DE STR BioSpectrometry Workstation, essentially as described previously (15). At least 200 spectra were collected and summarized for each sample. The method was optimized for glycan analysis in the used *m/z* range, and the mass accuracy was at least 0.2 Da. For the quantitative glycan profile analyses, mass spectrometric raw data were cleaned by carefully removing the effect of isotopic pattern overlapping, multiple alkali metal adduct signals, products of elimination of water from the reducing oligosaccharides, and other interfering mass spectrometric signals not arising from the original glycans in the sample. The resulting cleaned profiles were normalized to 100% to allow comparison between samples (16). To validate the relative quantitation approach, we analyzed analyte-signal and signal-response rates at different *m/z* areas of the mass spectrometric glycan profile with standard glycan mixtures.

Quantitative difference between two glycan profiles was calculated according to Eq. A:

$$difference = \frac{1}{2}\sum_{i=1}^{n}\left|p_{i,a} - p_{i,b}\right|, \quad \text{(A)}$$

where p is the relative abundance (%) of glycan signal i in profile a or b, and n is the total number of glycan signals in the profile.

Exoglycosidase digestions. All exoglycosidase reactions were done essentially as described (15) and the results were analyzed by MALDI-TOF mass spectrometry. Control digestions with characterized oligosaccharides were done in parallel with the analytic exoglycosidase reactions. The enzymes were *A. ureafaciens* neuraminidase (recombinant in *E. coli*; Glyko), *S. pneumoniae* β-*N*-acetylglucosaminidase (recombinant in *E. coli*; Calbiochem), *S. pneumoniae* β1,4-galactosidase (recombinant in *E. coli*; Calbiochem), and α-mannosidase from Jack beans (*C. ensiformis*; Sigma).

GlcNAc expression degree calculation. The GlcNAc expression degrees were calculated from the relative abundancies of glycan signals **12**, **17**, and **21** in neutral glycan fractions. The nonreducing terminal groups of these glycan components were previously determined as either GlcNAc according to sensitivity to digestion with β-*N*-acetylglucosaminidase (**12** and **17**) or galactosylated GlcNAc according to sensitivity to β1,4-galactosidase digestion (**17** and **21**). The GlcNAc expression degree (GD) was calculated as the fraction of terminal GlcNAc groups of the total terminal groups, according to Eq. B:

$$GD = \frac{2\times(\mathbf{12}) + (\mathbf{17})}{2\times(\mathbf{12}+\mathbf{17}+\mathbf{21})}\times 100\% \quad \text{(B)}$$

where **12**, **17**, and **21** are relative abundances of glycan signals (Table 1).

Synthesis of UDP-GalN-biotin. The synthesis protocol has been described in detail previously (17). Briefly, uridine-5′-diphospho (2-amino-2-deoxy)-D-galactose (UDP-GalN) was synthesized from UDP-glucose and galactosamine-1-phosphate with galactose-1-phosphate uridyltransferase (E.C. 2.7.7.12; Sigma; ref. 18), after which the product was reacted with sulfosuccinimidyl-6-(biotinamido)hexanoate (sulfo-NHS-LC-biotin; Pierce). The resulting product, uridine-5′-diphospho *N*-(6-biotinamidohexanoyl)-(2-amino-2-deoxy)-D-galactosamine (UDP-GalN-biotin), was chromatographically purified to homogeneity and characterized by MALDI-TOF mass spectrometry and ^{1}H nuclear magnetic resonance spectroscopy (NMR).

Labeling of terminal GlcNAc residues with UDP-[^{14}C]Gal and UDP-GalN-biotin. The radioactive label was transferred from UDP-[^{14}C]Gal (Amersham) to terminal GlcNAc–containing acceptors with bovine milk β1,4-galactosyltransferase (Calbiochem). The biotin label was transferred from UDP-GalN-biotin with a recombinant β1,4-galactosyltransferase similar to the enzyme described previously (19). In a typical procedure, deparaffinized formalin-fixed and paraffin-embedded tissue sections were incubated at 37°C with a reaction mixture containing 10 mmol/L UDP-GalN-biotin, 160 to 200 μmol/min/L enzyme, 100 mmol/L Tris-HCl or 50 mmol/L Na-MOPS (pH 7.4), and 20 mmol/L $MnCl_2$. After washing, the radioactive label was visualized by autoradiography, and the biotin groups were visualized by fluorescein-labeled streptavidin (Pharmingen) and fluorescence microscopy. Alkali treatment of tissue sections was accomplished with concentrated ammonia at 60°C. The details of the enzymatic labeling on thin-layer chromatograms are described in Supplementary Data.

Statistical analysis. Statistical analyses were done with the SAS Software (SAS System, version 8.2, SAS Institute, Inc.) using SAS/STAT and SAS/BASE modules. All tests were done as two-sided. The distributions of the experimental data were evaluated as (*a*) normal and symmetrical, (*b*) only symmetrical, or (*c*) nonsymmetrical and not normal, and the statistical test used was accordingly chosen as (*a*) Student's *t* test, (*b*) Wilcoxon signed rank test, or (*c*) sign test. $P < 0.05$ was considered statistically significant.

Results

Mass spectrometric analysis of the protein-linked glycome. To study the global cancer-associated changes in glycoprotein glycosylation, we used archived paraffin-embedded tissue samples from cancer patients. The sample panel consisted of various tumor types, and each tumor sample was accompanied by corresponding normal tissue sample from the same patient. After morphologic identification of relevant areas in the tissue samples (Fig. 1*A* and *B*), they were dissected for glycan analysis.

Glycoprotein glycan structures are preserved intact in formalin-fixed and paraffin-embedded archival tissue samples (20). In the present study, protein-linked glycans were detached from deparaffinized archival tissue sections, purified, and analyzed by MALDI-TOF mass spectrometry (Fig. 1*C*). The applied chemical glycan detachment method (11) was based on the use of strong alkaline conditions where both serine- and threonine-linked glycans (i.e., *O*-glycans; ref. 21) and asparagine-linked glycans (i.e., *N*-glycans; ref. 22) were liberated. The chemical isolation method also allowed uniform glycan liberation from tissue sections.

The relative intensities of glycan signals in MALDI-TOF mass spectrometry reflect their molar proportions in the sample (23–25), enabling comparative analyses of glycan profiles recorded from different samples. The relative abundance of each glycan signal was expressed as "percentage of the total profile" (16). Various methods for glycan profiling have been described (27, 28).[6] In the present work, the glycans were analyzed directly after isolation as nonderivatized reducing oligosaccharides. This procedure was straightforward and sensitive for the small tumor samples to be analyzed—in the order of ~1 mm^3 of tissue and low picomolar amounts of isolated glycans.

Figure 2 shows the MALDI-TOF mass spectrometric profiles of the major neutral protein-linked glycans from paraffin-embedded archival tissue samples of lung small-cell carcinoma and unaffected part of the same lung. The neutral glycan fraction comprised

[6] Consortium for Functional Glycomics (http://www.functionalglycomics.org).

Published OnlineFirst July 7, 2009; DOI: 10.1158/0008-5472.CAN-08-0289

Table 1. Sample characteristics and terminal GlcNAc expression data in human carcinomas

	Terminal GlcNAc in *N*-glycan antennae (%)*				
Lung cancer patient	Normal	Malignant tumor	Type	Stage †	Age and gender
Patient 1 (Figs. 2–4)	58	84	SCC	$T_1N_1M_0$	72 F
Patient 2	35	54	Adenoca	$T_2N_1M_0$	53 M
Patient 3	49	56	Adenoca	$T_3N_0M_0$	62 M
Patient 4	61	78	Adenoca	$T_2N_0M_0$	58 M
Patient 5	46	71	SCC	$T_2N_0M_0$	63 F
Patient 6	61	65	SCC	$T_1N_0M_0$	76 M
Patient 7	36	51	SCC	$T_2N_1M_0$	50 M
Average, $n = 7$	51	67			
Wilcoxon signed rank test		$P = 0.0156 < 0.05$			
Cancer type	Normal	Malignant tumor	n		GlcNAc ‡
Renal cell carcinoma	58	69	5		+
Ductal breast carcinoma	39	47	11		+
Lobular breast carcinoma	49	52	7		—
Ovarian adenocarcinoma	56	64	11		+§
Colon carcinoma	51	52	6		—
Pancreatic carcinoma	57	51	3		+/—‖
Gastric carcinoma	58	37	6		—
Hepatocellular carcinoma	63	61	1		—
Laryngeal carcinoma	46	62	1		+

NOTE: Top: lung cancer data of the small-cell carcinoma and lung adenocarcinoma patients. Bottom: other studied cancer types.
Abbreviations: SCC, small-cell carcinoma; Adenoca, adenocarcinoma.
*GlcNAc degree was calculated as described in Materials and Methods.
†TNM staging according to Lababede and colleagues (49).
‡+, accumulating terminal GlcNAc; —, not accumulating terminal GlcNAc on average (individual variation was observed).
§GlcNAc degree was 51 for benign ovarian adenomas (average; $n = 12$), showing no accumulation of terminal GlcNAc in benign tumors.
‖One of the three pancreatic carcinoma patients showed intense accumulation of terminal GlcNAc.

~50% of the detected protein-linked glycans in the human lung sample, the rest being acidic sialylated glycans (data not shown). The present neutral glycan profiles included signals that were expressed in both samples (invariable glycans) as well as signals that were more abundant in the tumor compared with the normal lung tissue (cancer-associated glycans; circled in Fig. 2*B*).

The major invariable glycan signals were **5**, **9**, **15**, **20**, and **23**, corresponding to monosaccharide compositions $Hex_{5\text{-}9}HexNAc_2$ (i.e., glycans that were composed of two *N*-acetylhexosamine residues and five to nine hexose residues; Fig. 2). To characterize the glycan structures, we treated the glycan sample with α-mannosidase enzyme and then analyzed the reaction products by mass spectrometry. Because the five glycan signals disappeared from the mass spectrum after enzymatic treatment, they could be assigned as high-mannose type *N*-glycans. The present results indicate that high-mannose type *N*-glycans are expressed uniformly in both normal tissues and malignant tumors of the lung as well as in all the other studied tumors and tissues. In both samples, their proportion of the observed signal intensity was 45% to 50% of the total neutral glycan profile. High-mannose type *N*-glycans are essential intermediates in human *N*-glycan biosynthesis (22), and therefore they are known to be expressed by all human cells.

To evaluate the magnitude of the cancer-associated glycome change, we calculated the total quantitative profile difference between normal and tumor tissue neutral *N*-glycan profiles (Fig. 2*A* and *B*). Altogether, the neutral glycan profiles differed by 24% from each other, which was a surprisingly large difference. The majority of this change was due to the change in the major cancer-associated glycan signal (**12**) corresponding to monosaccharide composition $Hex_3HexNAc_4dHex_1$. The relative abundance of this glycan signal was approximately six times higher in the tumor sample than in normal lung tissue. In addition, glycan signals **4**, **6**, **8**, and **17** (circled in Fig. 2*B*) had higher signal intensities in the tumor than in the normal lung (Fig. 2*D*). A common feature in the monosaccharide compositions of all these tumor associated glycan signals was a higher HexNAc:Hex ratio compared with normal lung neutral protein-linked glycans. In other words, the tumor-associated glycans contained more HexNAc residues per molecule compared with a typical normal human lung glycan. These results indicated that the glycans that were specifically accumulating in the lung tumor had a common structural feature.

Structural characterization of the lung cancer-associated glycans. To characterize the molecular structures of the cancer-associated glycan signals, the tumor glycans were first treated with specific exoglycosidase enzymes. Because the interesting glycans contained additional HexNAc residues, β-hexosaminidase enzymes were used. On specific β-*N*-acetylglucosaminidase (29) treatment of the lung cancer neutral glycan sample (Fig. 2*C*), various glycan signals were transformed into signals at lower mass-to-charge ratio (*m/z*), indicating the presence of either one or two nonreducing

Published OnlineFirst July 7, 2009; DOI: 10.1158/0008-5472.CAN-08-0289

terminal β-*N*-acetyl-D-glucosamine (GlcNAc) residues (arrows in Fig. 2*C*): **4** (one), **6** (one), **8** (two), **12** (two), and **17** (one). The major tumor-associated glycan signals were thus shown to contain a common structural feature: presence of nonreducing terminal GlcNAc residues.

The molecular structure of the major cancer-associated glycan signal **12** was further characterized by a combination of methods, including sequential treatments with β-*N*-acetylglucosaminidase, α-mannosidase, β-mannosidase, and endoglycosidase F1 (30); isolation by *N*-glycosidase F from the tumor tissue samples (31); and mass spectrometric analyses (see details in Supplementary Data). Taken together, the evidence indicated that glycan signal **12** consisted of complex-type *N*-glycan with the experimental molecular structure (GlcNAcβManα)$_2$Manβ4GlcNAcβ4(Fucα6)GlcNAc(β-N-Asn), where the terminal GlcNAc residues are underlined and Asn indicates the original linkage to asparagine residues in tumor glycoproteins (Fig. 4*A*).

By analyzing the sialylated glycan fractions of lung cancer tissue samples, it was confirmed that the observed increase in GlcNAc expression in the tumor neutral glycan fraction was not due to increased sialylation. Moreover, β1,4-galactosidase enzyme treatment of the isolated glycans showed that glycan signals **17** and **21** correspond to galactosylated forms of glycan signal **12** (Supplementary Data). The observed increase in the amounts of glycan signal **12** was therefore attributable to decreased galactosylation of protein-linked glycans in the tumor.

Occurrence of protein-linked GlcNAc glycans in human cancers. For a group of seven patients with lung carcinomas, terminal GlcNAc expression levels were calculated based on the relative intensities of glycan signals **12**, **17**, and **21** in each sample (Table 1). All tumor samples in this group showed an increase in GlcNAc expression when compared with the normal lung samples from the same patients. The difference was statistically significant between the tumor and normal tissue sample pairs with $P < 0.05$ ($P = 0.0156$, Wilcoxon signed rank test; $n = 7$). Of the seven tumors, four were small-cell carcinomas and three were adenocarcinomas. No significant differences were found between the two patient groups in the present experiments.

A panel of major human cancer types was screened by mass spectrometric analysis for increased amounts of terminal GlcNAc residues in the protein-linked glycans of archival tissue samples (Table 1). The mass spectrometric glycan signal **12** was increased in

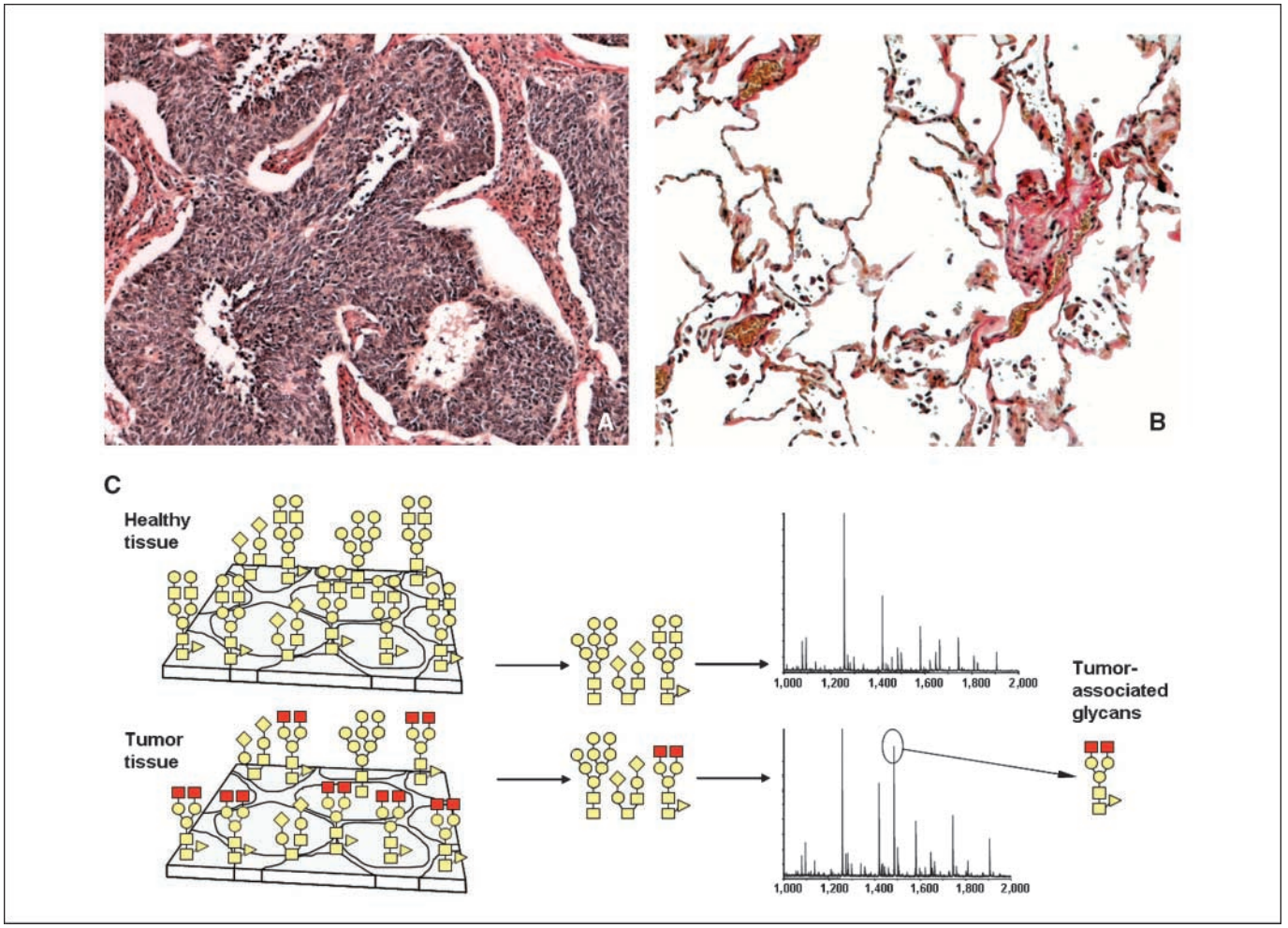

Figure 1. Glycome analysis of archival cancer patient tissue sections by mass spectrometric protein-linked glycan profiling. *A* and *B*, morphology of region of small-cell carcinoma (*A*) and normal lung tissue (*B*) from a patient that was analyzed in the present experiments. *C*, outline of the analysis method. About 1 mm^3 of archival tissue with intact preserved glycans (*left*) is cut into 20-μm sections and protein-linked glycans are detached chemically. The detached glycans (*middle*)

Published OnlineFirst July 7, 2009; DOI: 10.1158/0008-5472.CAN-08-0289

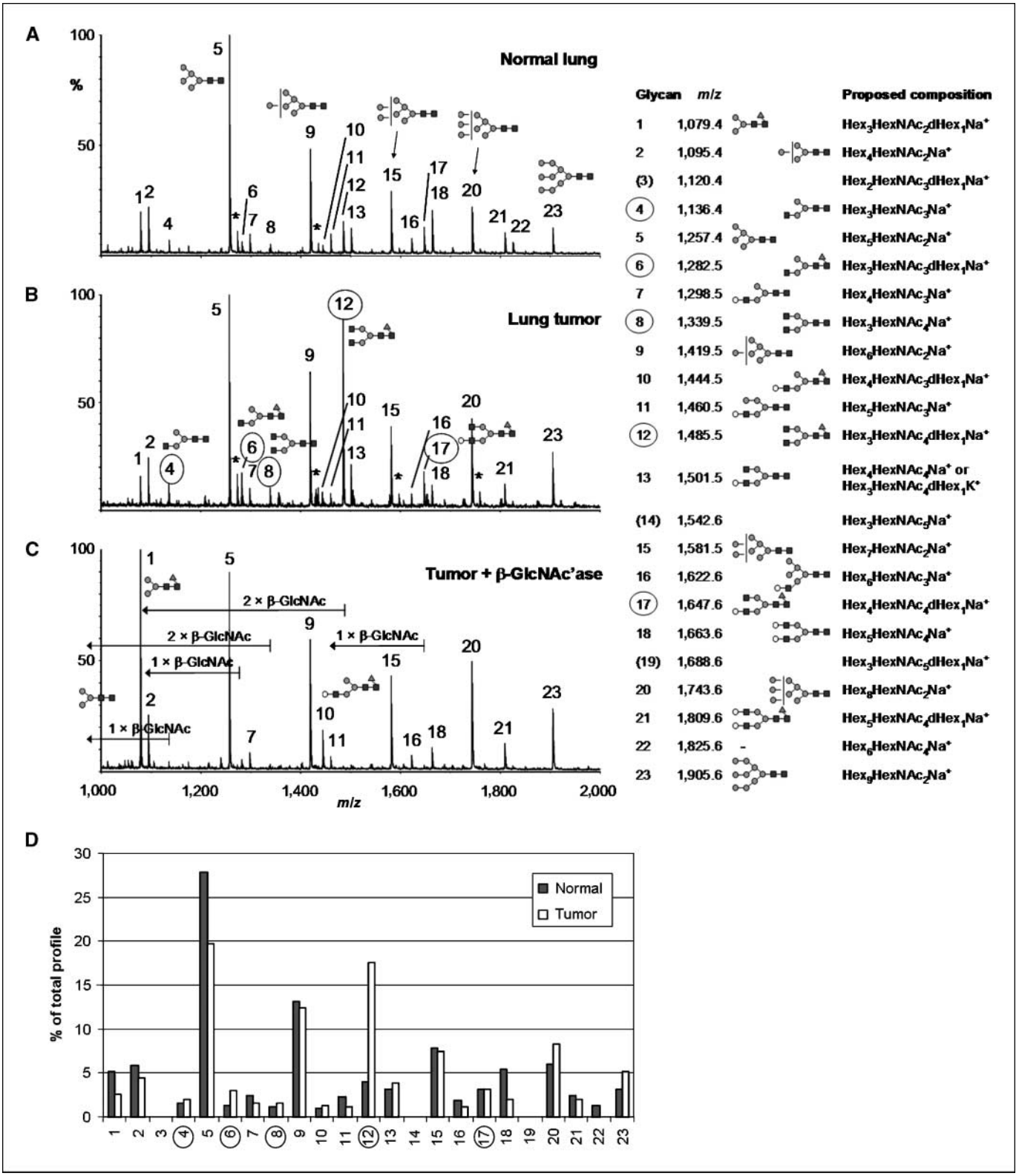

Figure 2. Identification of lung cancer-associated glycan antigens. *A* and *B,* MALDI-TOF mass spectrometric profiles of neutral protein-linked glycans between *m/z* 1,000 and 2,000 Da, isolated from paraffin-embedded archival tissue samples of normal lung tissue (*A*) or lung small-cell carcinoma (*B*). *C,* the lung cancer glycan sample was treated with β-*N*-acetylglucosaminidase enzyme to reveal glycans with nonreducing terminal GlcNAc residues. The enzyme digested glycan signals **4**, **6**, **8**, **12**, and **17** into smaller fragments (*arrows*), indicating the presence of either one or two terminal GlcNAc in these signals. *D,* column diagram of the mass spectrometric glycan profiles of *A* and *B* normalized to 100% of total profile allowing comparison of relative signal intensities. *y*-axis: relative signal intensity, 0% to 100%; *x*-axis: *m/z* ratio. *Asterisks,* potassium adduct ions. The glycan signal numbering for each *m/z* and the corresponding proposed composition of the glycan adduct ions are described on the right. Signals occurring only in Supplementary Data are in parentheses. Major glycans are represented by schematic figures: *squares,* GlcNAc; *grey circles,* mannose; *open circles,* galactose; *triangles,* fucose.

Published OnlineFirst July 7, 2009; DOI: 10.1158/0008-5472.CAN-08-0289

all cancer types overexpressing terminal GlcNAc glycans. Terminal GlcNAc was associated with the analyzed lung, renal cell, ovarian, pancreatic, and ductal breast carcinomas, but not with colon, gastric, hepatocellular, laryngeal, or lobular breast carcinomas. On the other hand, in all the studied patient samples, GlcNAc glycans were also detected in the control tissues. These results further showed that whereas the amounts of these glycan antigens were increased in certain cancer types, they were also present in the normal human glycome.

Targeting of GlcNAc-expressing tumors with galactosyltransferase probe. β1,4-Galactosyltransferase enzyme covalently transfers galactose (Gal) from uridine diphosphogalactose (UDP-Gal) to terminal GlcNAc residues with high specificity (32). To perform a histochemical analysis of terminal GlcNAc expression in the archival tissue specimens, tissue sections were radioactively labeled with ^{14}C-labeled UDP-Gal and β1,4-galactosyltransferase (Fig. 3*A*). To decrease background staining influenced by intercellular O-GlcNAc glycosylation (33), the tissue sections were alkali treated before the labeling. Autoradiography revealed a clear difference between tumor and normal tissue samples from the same patient as above (Fig. 3*B*), indicating increased amounts of terminal GlcNAc residues in the tumor sample. In accordance with

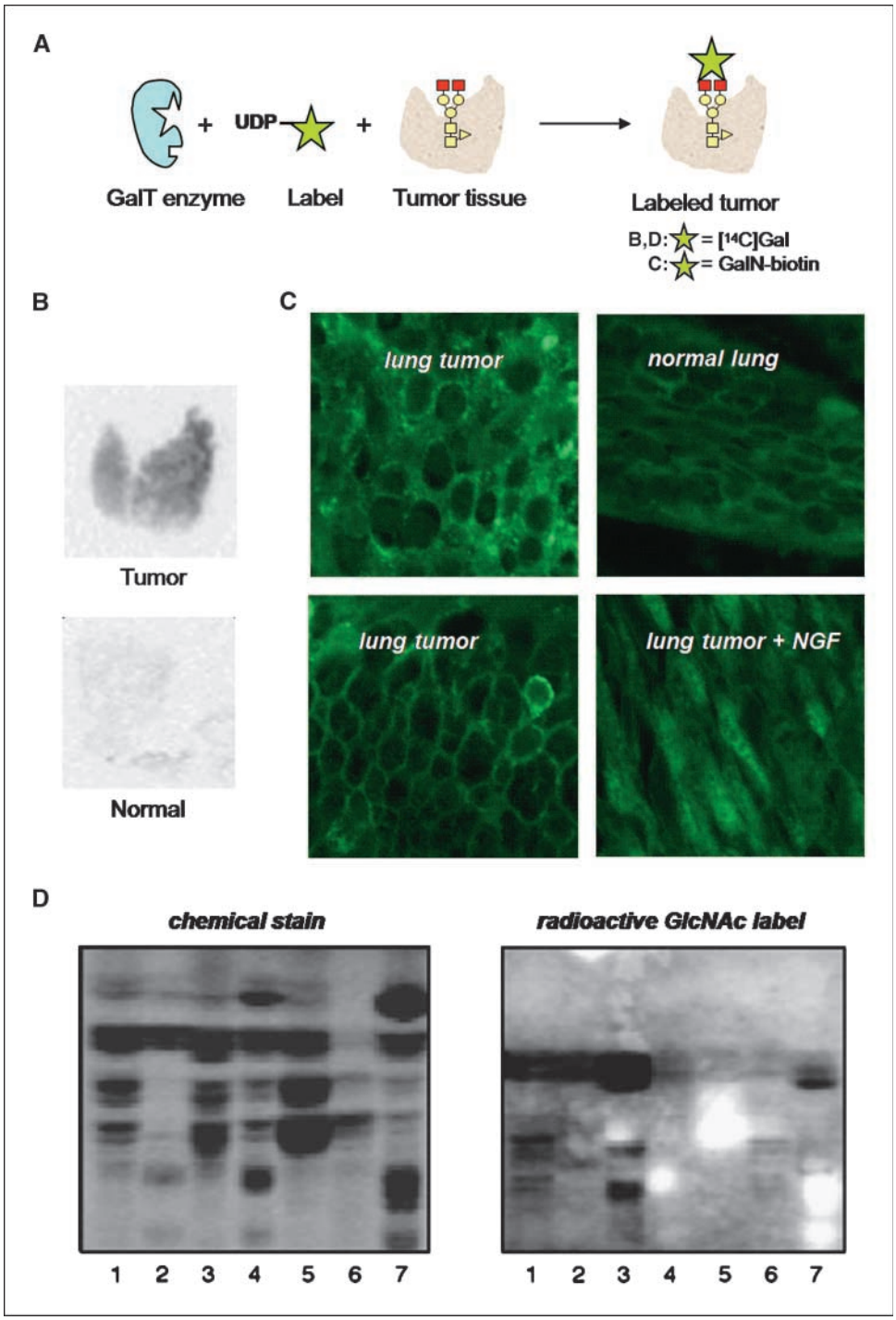

Figure 3. *A,* covalent labeling of terminal GlcNAc glycans in human cancer samples by GlcNAc-specific β1,4-galactosyltransferase enzyme. *B,* glycoproteins were radioactively labeled and detected with autoradiography in formalin-fixed and deparaffinized tissue sections of lung small-cell carcinoma (*top*) and normal lung tissue from the same patient (*bottom*). *C,* terminal GlcNAc–specific biotin labeling of tumor cell borders was visualized by fluorescence microscopy. Staining was intense and localized to cell borders in different areas of lung small-cell carcinoma (*left*), whereas in adjacent normal lung tissue the staining was weaker (*top right*). *N*-glycosidase F enzyme digestion of the tumor tissue sections removed the cell border–associated staining (*bottom right*), indicating that the cancer-associated terminal GlcNAc occurred mainly in *N*-glycans. *D,* glycolipids were labeled in thin-layer chromatograms with separated glycosphingolipids detected with anisaldehyde (*left*) and autoradiography (*right*). The lanes represent non-acid glycosphingolipids isolated from gallbladder adenocarcinoma (*lane 1*), colon adenocarcinoma metastasis (*lanes 2, 4*, and *7*), lung cancer metastasis (*lane 3*), and renal cell carcinoma (*lanes 5* and *6*).

Published OnlineFirst July 7, 2009; DOI: 10.1158/0008-5472.CAN-08-0289

previous results, the labeling of the normal tissue was weak (34). Thus, the differences observed in the mass spectrometric analyses of tumor and normal specimens correlated with radiohistochemical staining of tissue sections. Furthermore, when the radiolabeled molecules were isolated from the tumor tissue section, their analysis showed that most of the radioactivity had been incorporated to glycans chromatographically identical to glycan signal **12** (Supplementary Data).

A novel reagent for specific biotinylation of terminal GlcNAc antigens was synthesized by covalent coupling of biotin to the amino group of uridine diphosphogalactosamine (UDP-GalN). The resulting UDP-GalN-biotin reagent was used with a specific β1,4-galactosyltransferase enzyme to transfer GalN-biotin to terminal GlcNAc glycans with similar specificity as in the radioactive labeling above. Figure 3*C* shows the results obtained by using the UDP-GalN-biotin reagent and specific β1,4-galactosyltransferase for biotinylation, then fluorescein-conjugated streptavidin and fluorescence microscopy for detection of the label. Carcinoma cells were labeled with this biotinylation reagent and the staining was localized to cancer cell borders (Fig. 3*C, left*), whereas the staining in adjacent normal lung tissue was weaker (Fig. 3*C, top right*). When the tissue sections were treated with *N*-glycosidase enzyme before the staining, specifically the cell border staining was lost (Fig. 3*C, bottom right*), showing that the majority of the terminal GlcNAc antigens were *N*-glycans, consistent with both mass spectrometric and radiochemical data discussed above.

Glycolipid structures with terminal GlcNAc. Because malignant human tumors were shown to express considerable amounts of abnormal terminal GlcNAc in protein-linked glycans, it was of interest to analyze if similar structures occurred also in lipid-linked glycans. Glycolipid structures with nonreducing terminal GlcNAc are not typical to the normal human glycome (35). To screen for glycosphingolipids with terminal GlcNAc in human tumors, non-acid glycosphingolipids isolated from fresh tumor tissues of various human cancer types were separated on thin-layer chromatograpy plates and incubated with β1,4-galactosyltransferase and ^{14}C-labeled UDP-Gal as described above for tissue sections (Fig. 3*D*). Radioactivity was incorporated in a fast-migrating band, most likely lactotriaosylceramide (GlcNAcβ3Galβ4GlcβCer, Fig. 4*B*), in all fractions. In addition, more slowly migrating bands were detected in the non-acid glycosphingolipid fractions from one gallbladder carcinoma (*lane 1*), two of three colon carcinoma metastases (*lanes 2* and *7*), one lung carcinoma metastasis (*lane 3*), and one of two renal cell carcinomas (*lane 6*). The results indicated that glycosphingolipids containing terminal GlcNAc antigens were present in all these human cancer types. The renal cell carcinoma specimen in *lane 6* was from a patient that also showed markedly elevated expression of protein-linked GlcNAc glycans, especially glycan signal **12** (data not shown).

The radioactively labeled non-acid glycosphingolipid subfractions isolated from renal cell carcinoma were studied in detail. Negative ion FAB mass spectrometry of the less complex of these fractions (see Supplementary Fig. S7, *lane 2*) showed glycosphingolipids with HexNAc-Hex-HexNAc-Hex-Hex-Cer and Hex-HexNAc-Hex-HexNAc-Hex-Hex-Cer sequences. By proton NMR, these glycosphingolipids were identified as GlcNAcβ3nLc$_4$Cer (Fig. 4*C*) and its galactosylated variant Galβ4GlcNAcβ3nLc$_4$Cer, respectively. The negative ion FAB mass spectrum of the more complex fraction (see Supplementary Fig. S7, *lane 4*) indicated three different glycosphingolipids with terminal GlcNAc residues that were characterized by proton NMR (Fig. 4*C* and *D*; details in Supplementary Data). Taken together, the results showed that terminal GlcNAc–containing glycolipids occurred in various human cancer types, and in some tumors, both glycoprotein and glycosphingolipid glycan structures simultaneously carried terminal GlcNAc antigens.

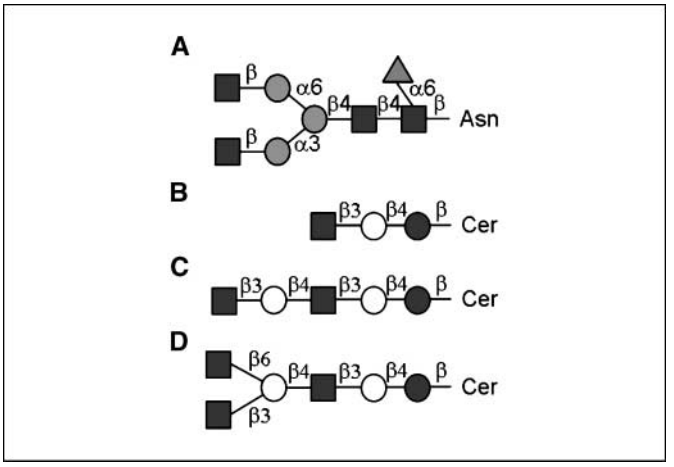

Figure 4. The major characterized glycans detected in malignant tumors expressing terminal GlcNAc antigens (*blue squares*). *A,* glycan **12** represents a glycoprotein *N*-glycan linked to asparagine residues (*Asn*) in tumor glycoproteins. *B,* lacto-*N*-triose glycosphingolipid. *C,* linear neolacto-*N*-pentose glycosphingolipid. *D,* branched glycosphingolipid containing two terminal GlcNAc units. *Cer,* ceramide. Monosaccharide symbols are as in Fig. 2.

Discussion

In the present report, we describe optimized methods for cancer glycomics, the analysis of cancer-associated glycan structures. The methods included isolation of nonderivatized glycans from paraffin-embedded tissue samples, MALDI-TOF mass spectrometric profiling of protein-linked glycans and parallel analysis of lipid-linked glycans, as well as covalent labeling of the tumor-associated glycan epitopes with a specific enzyme. The mass spectrometric glycan analysis method was developed for rapid detection of differentially expressed protein-linked glycans in tumor and control samples. This approach can be described as "glycan fingerprinting." The quantitatively processed glycan profiles further allowed statistical analyses.

The difference between neutral protein-linked glycan profiles of lung carcinoma and normal lung tissue was here determined to be ~25%. In addition, all the malignant tumor samples analyzed in the present study had altered glycan profiles (altogether more than 50 patient sample pairs in 10 cancer indications). An important conclusion of the present results is that a significant change in the tissue glycome is a characteristic feature of malignant tumors.

We found that a common structural feature, terminal β-*N*-acetyl-D-glucosamine (GlcNAc), was characteristic of a group of protein- and lipid-linked glycans overexpressed especially in malignant tumors of the lung (small-cell carcinoma and adenocarcinoma), kidney (renal cell carcinoma), breast (ductal carcinoma), and ovary (adenocarcinoma). A common glycosylation machinery is overlapping in both glycoprotein and glycolipid biosynthesis, and several metabolic and catabolic enzymes may account for the increased terminal GlcNAc expression detected in the present study (36). The genetic and biochemical mechanisms

Published OnlineFirst July 7, 2009; DOI: 10.1158/0008-5472.CAN-08-0289

leading to this phenomenon and their relationship to cancer biology should be analyzed in a further study.

Terminal GlcNAc antigens have been shown to be very rare on human cell surfaces (34, 35), and in the present study, the GlcNAc antigens were observed to be associated with tumor cell surfaces. The present results suggest that reduced galactosylation of glycans may lead to exposure of terminal GlcNAc antigens on the cancer cell surfaces in human tumors, and that the accumulation of these glycans may become a major determinant in the tumor glycome. The present report is the first to describe such terminal GlcNAc glycan structures in solid tumors. The presence of linear GlcNAc-terminated glycosphingolipids in human leukemia cells has been reported (35), but the association of branched GlcNAc-terminated glycosphingolipids with human cancer is a novel discovery (Fig. 4*D*).

The major cancer-associated protein-linked *N*-glycan described in the present study (glycan **12** in Figs. 2 and 4*A*) is a common biosynthetic intermediate in complex-type *N*-glycan biosynthesis (22) that occurs inside human cells in the Golgi complex, and the same structure is present, for example, in human serum IgG (37). We cannot rule out that a fraction of detected terminal GlcNAc expressing *N*-glycans were derived from serum glycoproteins. However, the most common IgG glycoform in healthy individuals is glycan **17** in Fig. 2 (37) and not glycan **12**, the major cancer-associated glycan detected in the present work. Recent reports have described potential glycan biomarkers in total serum *N*-glycome analyses. The published serum cancer marker lists have included glycan **12** in serum of breast (10) and prostate cancer patients (38). Nevertheless, the detected glycosphingolipid structures with terminal GlcNAc suggest that the accumulation mechanisms are at least partly endogenous to the tumors rather than contamination from serum glycoproteins. Further, the present GlcNAc-specific histochemistry data localized the tumor-associated GlcNAc antigens on the borders of tumor cells (Fig. 3*C*). Such localization could make the tumor GlcNAc antigens attractive targets to cancer-targeting strategies.

Identification of cancer-specific glycan structures can be useful in the development of new cancer therapies, for example, in generation of vaccines or antibodies targeting tumor-associated glycan antigens (39–43). Previous studies have shown antitumor immune responses against terminal GlcNAc-type structures in animal models (44, 45). However, the relevance of these reports with regard to human cancer should be studied further due to species specificity of glycosylation. By using synthetic oligosaccharides as ligands, we observed that natural human antibodies specific for terminal GlcNAc antigens are present in human serum, which suggests that GlcNAc antigens are immunogenic in humans.[7] We suggest that immunotherapy against the chemically defined cancer-associated glycan structures with terminal GlcNAc epitopes (Fig. 4) should be evaluated in experimental models of cancer therapy.

The present results also indicate that mass spectrometric glycome analysis could be used as a diagnostic or prognostic method in cancer diagnostics. Examples of the potential of glycan analysis in diagnostics have been reported (10, 38, 46), but mass spectrometric analysis of the glycome has, to date, not yet been applied in clinical diagnostics. As discussed above, recent reports have shown that the presence of malignant tumors in the human body may be reflected in the serum glycan profile, which gives hope for applications of glycomic analysis in cancer diagnostics in the future. The present method that uses microscale solid-phase extraction for purification of nonderivatized glycans could be easily incorporated to existing procedures and equipment developed for proteomics-based diagnostics.

Based on the molecular structures of the cancer-associated glycans, a specific enzymatic method was designed for the targeting of isotope or biotin label to tumor-associated glycan structures. The glycan-specific labeling of tumor tissues was shown to correlate with mass spectrometric analysis results. Methods that use the same enzymatic activity have been published for tagging O-linked GlcNAc glycans *in vitro* (47) and for enabling preservation of platelets in the cold (48). Given the scarce expression of cell surface GlcNAc antigens in normal tissues, the present method might also be applicable for covalent labeling of tumors *in vivo*.

[7] Unpublished preliminary data.

Disclosure of Potential Conflicts of Interest

T. Satomaa, J. Natunen, and J. Saarinen are shareholders of Glykos Finland Ltd. T. Satomaa, A. Heiskanen, A. Olonen, N. Salovuori, S. Teneberg, J. Natunen, and J. Saarinen are inventors in patent applications related to the present work. The other authors disclosed no potential conflicts of interest.

Acknowledgments

Received 4/10/08; revised 3/19/09; accepted 5/18/09; published OnlineFirst 7/7/09.

Grant support: The Finnish Funding Agency for Technology and Innovation, TEKES (to Glykos Finland Ltd.), the Swedish Medical Research Council (S. Teneberg), the Swedish Cancer Foundation (S. Teneberg), and the Swedish Medical Society/The Foundations of the National Board of Health and Welfare (S. Teneberg).

The costs of publication of this article were defrayed in part by the payment of page charges. This article must therefore be hereby marked *advertisement* in accordance with 18 U.S.C. Section 1734 solely to indicate this fact.

We thank I. Pasanen and E. Löyttyniemi for statistical analyses and H. Valo, M. Reinman, and Biotie Therapies Corp. Plc. (Turku, Finland) for help.

References

1. Fuster MM, Esko JD. The sweet and sour of cancer: glycans as novel therapeutic targets. Nat Rev Cancer 2005;5:526–42.
2. Hakomori S. Cancer-associated glycosphingolipid antigens: their structure, organization, and function. Acta Anat (Basel) 1998;161:79–90.
3. Brockhausen I. Biosynthesis and functions of *O*-glycans and regulation of mucin antigen expression in cancer. Biochem Soc Trans 1997;25:871–4.
4. Springer GF. Immunoreactive T and Tn epitopes in cancer diagnosis, prognosis, and immunotherapy. J Mol Med 1997;75:594–602.
5. Dennis JW, Granovsky M, Warren CE. Glycoprotein glycosylation and cancer progression. Biochim Biophys Acta 1999;1473:21–34.
6. Dube DH, Bertozzi CR. Glycans in cancer and inflammation-potential for therapeutics and diagnostics. Nat Rev Drug Discov 2005;4:477–88.
7. Klinger M, Farhan H, Just H, et al. Antibodies directed against Lewis-Y antigen inhibit signaling of Lewis-Y modified ErbB receptors. Cancer Res 2004;64:1087–93.
8. Partridge EA, Le RC, Di Guglielmo GM, et al. Regulation of cytokine receptors by Golgi *N*-glycan processing and endocytosis. Science 2004;306:120–4.
9. Lowe JB, Marth JD. A genetic approach to mammalian glycan function. Annu Rev Biochem 2003;72:643–91.
10. Kyselova Z, Mechref Y, Kang P, et al. Breast cancer diagnosis and prognosis through quantitative measurements of serum glycan profiles. Clin Chem 2008;54:1166–75.
11. Huang Y, Mechref Y, Novotny MV. Microscale nonreductive release of O-linked glycans for subsequent analysis through MALDI mass spectrometry and capillary electrophoresis. Anal Chem 2001;73:6063–9.
12. Verostek MF, Lubowski C, Trimble RB. Selective organic precipitation/extraction of released *N*-glycans following large-scale enzymatic deglycosylation of glycoproteins. Anal Biochem 2000;278:111–22.
13. Davies MJ, Smith KD, Carruthers RA, Chai W, Lawson AM, Hounsell EF. Use of a porous graphitised carbon column for the high-performance liquid chromatography of oligosaccharides, alditols and glycopeptides with

subsequent mass spectrometry analysis. J Chromatogr 1993;646:317–26.
14. Slomianny M-C, Morelle W. In-gel release of N-linked carbohydrates from glycoproteins with analysis by matrix-assisted laser desorption/ionisation (MALDI) mass spectrometry. Sigma Origins 2004;13:4–5.
15. Saarinen J, Welgus HG, Flizar CA, Kalkkinen N, Helin J. *N*-glycan structures of matrix metalloproteinase-1 derived from human fibroblasts and from HT-1080 fibrosarcoma cells. Eur J Biochem 1999;259:829–40.
16. Aoki K, Perlman M, Lim JM, Cantu R, Wells L, Tiemeyer M. Dynamic developmental elaboration of N-linked glycan complexity in the *Drosophila melanogaster* embryo. J Biol Chem 2007;282:9127–42.
17. Natunen J, Teneberg S, Karlsson K-A, Satomaa T, Heiskanen A, inventors; Tumor specific oligosaccharides and use thereof. WO 2004/017810.
18. Hayashi T, Murray BW, Wang R, Wong CH. A chemoenzymatic synthesis of UDP-(2-deoxy-2-fluoro)-galactose and evaluation of its interaction with galactosyltransferase. Bioorg Med Chem 1997;5:497–500.
19. Ramakrishnan B, Qasba PK. Structure-based design of β1,4-galactosyltransferase I (β4Gal-T1) with equally efficient *N*-acetylgalactosaminyltransferase activity: point mutation broadens β4Gal-T1 donor specificity. J Biol Chem 2002;277:20833–9.
20. Dwek MV, Brooks SA, Streets AJ, Harvey DJ, Leathem AJ. Oligosaccharide release from frozen and paraffin-wax-embedded archival tissues. Anal Biochem 1996;242:8–14.
21. Hanisch FG. O-glycosylation of the mucin type. Biol Chem 2001;382:143–9.
22. Kornfeld R, Kornfeld S. Assembly of asparagine-linked oligosaccharides. Annu Rev Biochem 1985;54:631–64.
23. Harvey DJ. Quantitative aspects of the matrix-assisted laser desorption mass spectrometry of complex oligosaccharides. Rapid Commun Mass Spectrom 1993;7:614–9.
24. Naven TJ, Harvey DJ. Effect of structure on the signal strength of oligosaccharides in matrix-assisted laser desorption/ionization mass spectrometry on time-of-flight and magnetic sector instruments. Rapid Commun Mass Spectrom 1996;10:1361–6.
25. Papac DI, Wong A, Jones AJ. Analysis of acidic oligosaccharides and glycopeptides by matrix-assisted laser desorption/ionization time-of-flight mass spectrometry. Anal Chem 1996;68:3215–23.
26. Block TM, Comunale MA, Lowman M, et al. Use of targeted glycoproteomics to identify serum glycoproteins that correlate with liver cancer in woodchucks and humans. Proc Natl Acad Sci U S A 2005;102:779–84.
27. Chen YJ, Wing DR, Guile GR, Dwek RA, Harvey DJ, Zamze S. Neutral *N*-glycans in adult rat brain tissue-complete characterisation reveals fucosylated hybrid and complex structures. Eur J Biochem 1998;251:691–703.
28. Sutton-Smith M, Morris HR, Grewal PK, et al. MS screening strategies: investigating the glycomes of knockout and myodystrophic mice and leukodystrophic human brains. Biochem Soc Symp 2002;69:105–15.
29. Kiyohara T, Terao T, Shioiri-Nakano K, Osawa T. Purification and characterization of β-*N*-acetylhexosaminidases and β-galactosidase from *Streptococcus* 6646 K. J Biochem 1976;80:9–17.
30. Anumula KR. Endo β-*N*-acetylglucosaminidase F cleavage specificity with peptide free oligosaccharides. J Mol Recognit 1993;6:139–45.
31. Altmann F, Schweiszer S, Weber C. Kinetic comparison of peptide: *N*-glycosidases F and A reveals several differences in substrate specificity. Glycoconj J 1995;12:84–93.
32. Berger EG, Rohrer J. Galactosyltransferase—still up and running. Biochimie 2003;85:261–74.
33. Hart GW, Housley MP, Slawson C. Cycling of O-linked β-*N*-acetylglucosamine on nucleocytoplasmic proteins. Nature 2007;446:1017–22.
34. Spillmann D, Finne J. Specific labeling of cell surface poly-*N*-acetyllactosamine glycans. Methods Enzymol 1989;179:270–5.
35. Hu J, Stults CL, Holmes EH, Macher BA. Structural characterization of intermediates in the biosynthetic pathway of neolacto glycosphingolipids: differential expression in human leukaemia cells. Glycobiology 1994;4:251–7.
36. Murrell MP, Yarema KJ, Levchenko A. The systems biology of glycosylation. Chembiochem 2004;5:1334–47.
37. Raju TS, Briggs JB, Borge SM, Jones AJ. Species-specific variation in glycosylation of IgG: evidence for the species-specific sialylation and branch-specific galactosylation and importance for engineering recombinant glycoprotein therapeutics. Glycobiology 2000;10:477–86.
38. Kyselova Z, Mechref Y, Al Bataineh MM, et al. Alterations in the serum glycome due to metastatic prostate cancer. J Proteome Res 2007;6:1822–32.
39. Brandlein S, Pohle T, Ruoff N, Wozniak E, Muller-Hermelink HK, Vollmers HP. Natural IgM antibodies and immunosurveillance mechanisms against epithelial cancer cells in humans. Cancer Res 2003;63:7995–8005.
40. Henry CJ, Buss MS, Hellstrom I, et al. Clinical evaluation of BR96 sFv-PE40 immunotoxin therapy in canine models of spontaneously occurring invasive carcinoma. Clin Cancer Res 2005;11:751–5.
41. Holmberg LA, Sandmaier BM. Vaccination with Theratope (STn-KLH) as treatment for breast cancer. Expert Rev Vaccines 2004;3:655–63.
42. Shriver Z, Raguram S, Sasisekharan R. Glycomics: a pathway to a class of new and improved therapeutics. Nat Rev Drug Discov 2004;3:863–73.
43. Ouerfelli O, Warren JD, Wilson RM, Danishefsky SJ. Synthetic carbohydrate-based antitumor vaccines: challenges and opportunities. Expert Rev Vaccines 2005;4:677–85.
44. Meichenin M, Rocher J, Galanina O, et al. Tk, a new colon tumor-associated antigen resulting from altered O-glycosylation. Cancer Res 2000;60:5499–507.
45. Monzavi-Karbassi B, Luo P, Jousheghany F, et al. A mimic of tumor rejection antigen-associated carbohydrates mediates an antitumor cellular response. Cancer Res 2004;64:2162–6.
46. Callewaert N, Van VH, Van HA, Laroy W, Delanghe J, Contreras R. Noninvasive diagnosis of liver cirrhosis using DNA sequencer-based total serum protein glycomics. Nat Med 2004;10:429–34.
47. Bulter T, Schumacher T, Namdjou DJ, Gutierrez GR, Clausen H, Elling L. Chemoenzymatic synthesis of biotinylated nucleotide sugars as substrates for glycosyltransferases. Chembiochem 2001;2:884–94.
48. Hoffmeister KM, Josefsson EC, Isaac NA, Clausen H, Hartwig JH, Stossel TP. Glycosylation restores survival of chilled blood platelets. Science 2003;301:1531–4.
49. Lababede O, Meziane MA, Rice TW. TNM staging of lung cancer. Chest 1999;115:233–5.

Cancer Research
The Journal of Cancer Research (1916–1930) | The American Journal of Cancer (1931–1940)

AACR American Association for Cancer Research

Analysis of the Human Cancer Glycome Identifies a Novel Group of Tumor-Associated *N*-Acetylglucosamine Glycan Antigens

Tero Satomaa, Annamari Heiskanen, Iréne Leonardsson, et al.

Cancer Res 2009;69:5811-5819. Published OnlineFirst July 7, 2009.